Neuropsychologia 173 (2022) 108290

Contents lists available at ScienceDirect

Neuropsychologia

journal homepage: www.elsevier.com/locate/neuropsychologia

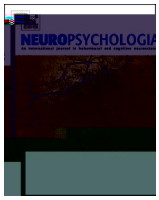

Ensemble size perception: Its neural signature and the role of global interaction over individual items

Jianrong Jia [a,b], Tongyu Wang [a,b], Siqi Chen [a,b], Nai Ding [c,d], Fang Fang [e,f,g,h,*]

[a] Center for Cognition and Brain Disorders, The Affiliated Hospital of Hangzhou Normal University, Hangzhou, 311121, China
[b] Institute of Psychological Sciences, Hangzhou Normal University, Hangzhou, 311121, China
[c] Key Laboratory for Biomedical Engineering of Ministry of Education, College of Biomedical Engineering and Instrument Sciences, Zhejiang University, Hangzhou, 311121, China
[d] Research Center for Advanced Artificial Intelligence Theory, Zhejiang Lab, Hangzhou, 311121, China
[e] School of Psychological and Cognitive Sciences and Beijing Key Laboratory of Behavior and Mental Health, Peking University, Beijing, 100871, China
[f] IDG/McGovern Institute for Brain Research, Peking University, Beijing, 100871, China
[g] Key Laboratory of Machine Perception (Ministry of Education), Peking University, Beijing, 100871, China
[h] Peking-Tsinghua Center for Life Sciences, Peking University, Beijing, 100871, China

ARTICLE INFO

Keywords:
Ensemble size
Steady-state visual evoked potential (SSVEP)
Temporal response function (TRF)
Global interaction
Local interaction

ABSTRACT

To efficiently process complex visual scenes, the visual system often summarizes statistical information across individual items and represents them as an ensemble. However, due to the lack of techniques to disentangle the representation of the ensemble from that of the individual items constituting the ensemble, whether there exists a specialized neural mechanism for ensemble processing and how ensemble perception is computed in the brain remain unknown. To address these issues, we used a frequency-tagging EEG approach to track brain responses to periodically updated ensemble sizes. Neural responses tracking the ensemble size were detected in parieto-occipital electrodes, revealing a global and specialized neural mechanism of ensemble size perception. We then used the temporal response function to isolate neural responses to the individual sizes and their interactions. Notably, while the individual sizes and their local and global interactions were encoded in the EEG signals, only the global interaction contributed directly to the ensemble size perception. Finally, distributed attention to the global stimulus pattern enhanced the neural signature of the ensemble size, mainly by modulating the neural representation of the global interaction between all individual sizes. These findings advocate a specialized, global neural mechanism of ensemble size perception and suggest that global interaction between individual items contributes to ensemble perception.

1. Introduction

The visual system has limited processing capacity (Luck and Vogel, 1997; Palmer et al., 2011). One strategy to overcome the capacity limitation and optimize information processing is to summarize the complex and redundant information into ensemble coding (Alvarez, 2011; Parkes et al., 2001; Whitney and Yamanashi Leib, 201). Our visual system is remarkably accurate in estimating ensemble properties (e.g., mean, variance) in multiple dimensions, including low-level visual features such as size (Ariely, 2001; Chong and Treisman, 200) and orientation (Parkes et al., 2001), and high-level visual characteristics such as emotion, gender (Haberman and Whitney, 2007), face identities (Neumann et al., 201), and biological motion (Sweeny et al., 201). However, because individual items constitute the ensemble, it is difficult for traditional neuroimaging methods to dissociate the neural process of ensemble perception from that of individual item perception. As a result, although ensemble perception has been studied extensively at the behavioral level over the past two decades, how it is implemented in the brain remains controversial.

Two hypotheses have been proposed to explain how ensemble perception is achieved in the brain. The subsampling hypothesis (yczek and Simons, 200; Simons and yczek, 200; Solomon et al., 2011) proposes that ensemble perception does not recruit a global mechanism; instead, it can be achieved by sampling and summarizing a subset of items. Specifically, a small subset of items are randomly sampled by attention, and their properties are averaged to generate a mean

* Corresponding author. School of Psychological and Cognitive Sciences, Peking niversity, 2 Haidian Road, Bei ing, 1000 7, China.
E-mail address: ffang pku.edu.cn (F. Fang).

https: doi.org 10.1011 .neuropsychologia.2022.10 290
Received 2 December 2021; Received in revised form 2 June 2022; Accepted 7 June 2022
Available online 10 June 2022

perception. Consequently, not all items in the stimulus set are processed in ensemble perception. The summary-statistic representation hypothesis (Ariely, 2001, 200; Chong et al., 200; Chong and Treisman, 200 a, 200 b), on the other hand, suggests a specialized global mechanism that computes summary-statistic representations over all displayed items. According to this hypothesis, the ensemble property of a stimulus set is processed in parallel with its individual items. All items are processed in the ensemble perception (Iakovlev and tochkin, 2021), although their weights may vary

approach to extract EEG responses specific to certain sensory stimulus inputs from the overall EEG recordings (Ding and Simon, 2012; Lalor et al., 2001). Here, to explore the neural representations and contributions of individual sizes and their interactions, we defined three components: individual sizes, their local interactions, and their global interaction. Operationally, the local interactions were defined as the products of two neighboring individual sizes and the global interaction between all individuals was defined as the product over eight individual sizes (im et al., 201 ; Werner and Noppeney, 2010). If the individual items interact with each other in the brain, the local and or global interaction components should be represented in the brain and contribute to the ensemble perception.

Previous studies have demonstrated that ensemble representation is enhanced when attention is distributed over the global pattern as opposed to when attention is focused on a single item (Baek and Chong, 2020a; Chong and Treisman, 200 b; de Fockert and archant, 200). It is unclear which components, individuals or their local or global interactions, are modulated by attentional distribution. odulating the attentional distribution provides a chance to explore which components are critical to ensemble perception. Therefore, Experiment 2 further investigated modulation of spatial attention distribution on ensemble perception. Taken together, the present study aims to address a series of questions regarding the neural mechanism of ensemble perception, including (1) the neural signature of ensemble size perception, (2) whether the individual sizes and their local and global interactions are represented in the brain and contribute to ensemble size perception, and ( ) whether the representations of individual sizes and their interactions are modulated by attentional distribution.

2. Materials and methods

2.1. Participants

A total of human volunteers (2 female, age range: 1–2 years) participated in this study. Experiment 1 (n = 2) and Experiment 2 (n = 22) were performed at Peking niversity and Hangzhou Normal niversity, respectively. Our sample sizes were comparable to those in recent studies using similar TRF methods (Broderick et al., 2019; Jia et al., 2017; O'Sullivan et al., 2019), which were typically from 11 to 20. We decided to recruit 2 and 22 participants for the two experiments because our data analysis would estimate 17 independent neural responses (see below) from the overall EEG signals. All participants were right-handed, reported normal or corrected-to-normal vision, and had no known neurological or visual disorders. They gave written, informed consent in accordance with the procedures and protocols approved by the Human Sub ect Review Committee of Peking niversity or Hangzhou Normal niversity.

2.2. Experiment 1

We used ATLAB (version 9. , The athWorks) and Psychotoolbox- extensions (Brainard, 1997; Pelli, 1997) to generate and display visual stimuli and record behavioral responses. The visual stimuli were presented on a Display++ LCD monitor (Cambridge Research Systems) with a 1920 × 10 0 spatial resolution and a 120 Hz refresh rate. Electroencephalography (EEG) recording was carried out in a dark room shielded from sound and electromagnetic signals. The participants were comfortably seated at 7 cm from the screen with their heads stabilized on a chin rest.

An array of circles were presented against a gray background (luminance: cd m^2) at eight fixed locations (Fig. 1a). The eccentricity of the center of each circle was 9° and the distance between ad acent circle centers was 1.9°. As depicted in Fig. 1, the edge of each circle consisted of an outer black line (luminance: 0. 1 cd m^2) and an inner white line (luminance: 107. 9 cd m^2), so that the mean luminance of each circle was equal to the background luminance.

A 1-s stimulus sequence consisted of 1 circle arrays, which were presented successively. Each circle array was presented for 1.7 ms (frame), so the sequence was updated at 2 Hz. The circle sizes in each array were determined independently using the following procedure (Fig. 1b). First, the radius of each of the eight circles was drawn from a uniform distribution between 0. ° and 1°. At the rd update of every updates, the mean radius of the eight circles was set to 0.9°, so that the mean size changed periodically at Hz (i.e., base frequency; Fig. 1b). In an oddball-present sequence, at the last update of every 2 updates, the mean radius of the eight circles was set to a larger size of 1.2° or 1. °, so that the oddball array appeared periodically at 1 Hz. Second, to enlarge the size differences among the circles in each array, n od

0. 7 s at a random time between 1 and 1 s after trial onset. The participants were asked to detect whether the circles were of the same size (the attend-to-ensemble condition), the changes in luminance of the fixation (the attend-to-fixation condition), and changes in contrast of the left circle (the attend-to-item condition) in three blocks respectively, by pressing a key. In each trial, a 1-s stimulus sequence was presented, and participants were instructed to maintain fixation on a small point at the center of the display. There was a 1–1. s interval between trials. The order of the blocks was counterbalanced across participants. At the beginning of each block, the participants completed trials to get familiar with the task. It took about 1 min to complete the whole experiment.

2.4. EEG data acquisition and processing

EEG signals were recorded continuously at 1000 Hz using two BrainAmp amplifiers and a 1 -channel EasyCap (BrainProducts). FCz electrode was used as reference and electrode impedances were maintained below kΩ during data acquisition. Horizontal and vertical electrooculograms were recorded by two additional electrodes around the sub ects' eyes. EEG signals were preprocessed using the FieldTrip toolbox (Oostenveld et al., 2011). They were re-referenced to the average value of all channels except two electrooculograms and were of ine band-pass filtered between 0.1 and 0 Hz using a Butterworth IIR filter with the order of 2. The signals were then downsampled to the same frequency as the screen refresh rate (i.e., 120 Hz in Experiment 1 and Hz in Experiment 2) for temporal response function (TRF) estimation (Lalor et al., 2001). Independent component analysis was performed to remove eye-movement and artifact components, and the remaining components were back-pro ected onto the EEG electrode space. 1-s EEG epochs during stimulus sequence presentation were segmented for each trial and used for further analyses.

2.5. SSVEP analysis

Evoked activities were computed by averaging EEG epochs for each condition and each participant. FFT was applied to the evoked activities after applying a Hanning taper to calculate the power spectrum for each channel with a frequency resolution (the size of the frequency bins) of 0.117 Hz. A baseline-correction procedure was used to extract SSVEP responses from baseline noise across the frequency spectrum (eigen and Bach, 2000). Specifically, the difference between the power in the bin of interest and the mean power in the six surrounding bins was computed. In Experiment 2, only the trials without any manipulation were included in the analysis to exclude the in uence of target detection on SSVEP.

2.6. Predicting EEG responses using individual circle sizes and their interactions as predictors

We used a forward TRF approach to predict EEG responses using individual circle sizes and their interactions as predictors. TRF describes the brain's linear transformation of the stimulus input, S(t), to the neural response output, R(t), as R(t) = TRF * S(t), where * denotes the convolution operator (Jia et al., 2017, 2019; Lalor et al., 2001). TRF was defined as a 1 s length neural response to each unit change in a predictor and was computed by a regularized linear regression between the predictor value and EEG amplitude. A parameter λ was used to control overfitting in the ridge regression.

In this study, we used eight circle sizes ($I_{1\text{-}8}$, they are I_1, I_2, I_3, I_4, I_5, I_6, I_7, I_8), eight local interactions ($L_{1\text{-}8}$, they are $I_1 \times I_2$, $I_2 \times I_3$, $I_3 \times I_4$, $I_4 \times I_5$, $I_5 \times I_6$, $I_6 \times I_7$, $I_7 \times I_8$, $I_8 \times I_1$) and a global interaction (G, that is $I_1 \times I_2 \times I_3 \times I_4 \times I_5 \times I_6 \times I_7 \times I_8$) to predict EEG responses (Best and Wolf, 201 ; Smith and utas, 201 ; Werner and Noppeney, 2010):

$$EEG = \left(\sum_{i=1}^{8} TRF_{Ii} \ * \ I_i\right) + \left(\sum_{i=1}^{8} TRF_{Li} * L_i\right) + TRF_G * G$$

where I_i and TRF_{Ii} are the size of the i-th circle and the corresponding TRF, L_i and TRF_{Li} are the i-th local interaction and the corresponding TRF, and G and TRF_G are the global interaction and the corresponding TRF. The individual size predictors represented the information of the eight circles, the local-interaction predictors represented the information of interactions between two neighboring individuals, and the global-interaction predictor represented the information of the highest-order interaction over all circles (Smith and utas, 201 ; Werner and Noppeney, 2010).

The TRF-based EEG prediction was performed using the multivariate temporal response function (mTRF) toolbox (ichael J. Crosse et al., 2011). The λ values in all models were set to 1 for all sub ects in our experiments. Each predictor was converted to z score before model fitting to reduce structural multicollinearity (Frost, 2019).

We quantified how well the individual circle sizes and their local and global interactions were encoded in the EEG signals using a leave-one-trial-out cross-validation procedure. TRFs were trained on N-1 trials and convolved with the predictors of the left-out trial to predict the channel-specific EEG signals (Broderick et al., 2019; Ding and Simon, 2012). The squared Pearson correlation coefficient (ichael J. Crosse et al., 2011; Frost, 2019) between the predicted and the recorded EEG signals were used to quantify the predicted accuracy (i.e., predicted R^2). The advantage of using predicted accuracy for model evaluation is that it is sensitive to model overfitting. Because it is impossible to predict random noise, the predicted accuracy must drop for an overfit model that adds random noise to the model as predictors (ichael J. Crosse et al., 2011; Frost, 2019). If the individual circle sizes and their interactions were encoded in the EEG signals, the predicted accuracy should increase after adding these predictors to the TRF model. We defined a full model using the individual circle sizes, local interactions, and global interaction as the predictors of the TRF model to predict the EEG signals (the *ILG* model) (see above). We then defined three reduced models that used the individual circle sizes and the local interactions (the *IL* model), the individual circle sizes and the global interaction (the *IG* model), or the local interactions and the global interaction (the *LG* model) as the predictors to predict the EEG signals, respectively. The encoding of

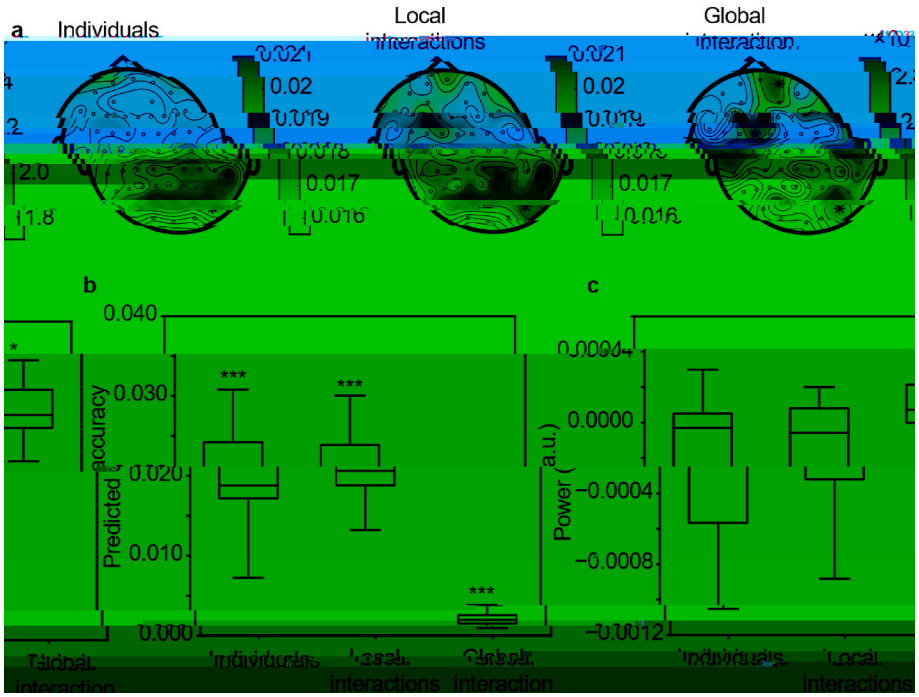

Fig. 3. Neural representation of the individual circle sizes, the local interactions, and the global interaction and their contributions to the SSVEP to the ensemble size. **a**. Topographies of predicted accuracy differences between the full and the three reduced models for quantifying the neural representation of the three predictors. Five electrodes with the best representation performance for each predictor, marked with asterisk, were selected for statistical analyses. **b**. Predicted accuracy differences between the full and the three reduced models, which were ascribed to the three predictors. **c**. Contributions of the three predictors to the SSVEP power. ***$p < 0.001$, *$p < 0.0$.

2 included three attention conditions: attend-to-ensemble, attend--to-fixation, and attend-to-item.

The response accuracies were 0.7 ± 0.0 , 0. ± 0.01, and 0.71 ± 0.0 for the attend-to-ensemble, attend-to-fixation, and attend-to-item conditions, respectively. There was no significant difference across the three conditions ($F(2, 2) = 2.19$, $p = 0.12$, partial $\eta^2 = 0.10$).

Replicating the findings in Experiment 1, the largest SSVEP power was observed also at the POz electrode (Fig.) and significant SSVEPs at the base frequency were found in all the three conditions (attend-to-ensemble: $W = 2\ 2$, $p < 0.001$, $r_{rb} = 0.99$; attend-to-fixation: $W = 2$, $p < 0.001$, $r_{rb} = 1.00$; attend-to-item: $W = 2\ 0$, $p < 0.001$, $r_{rb} = 0.9$).

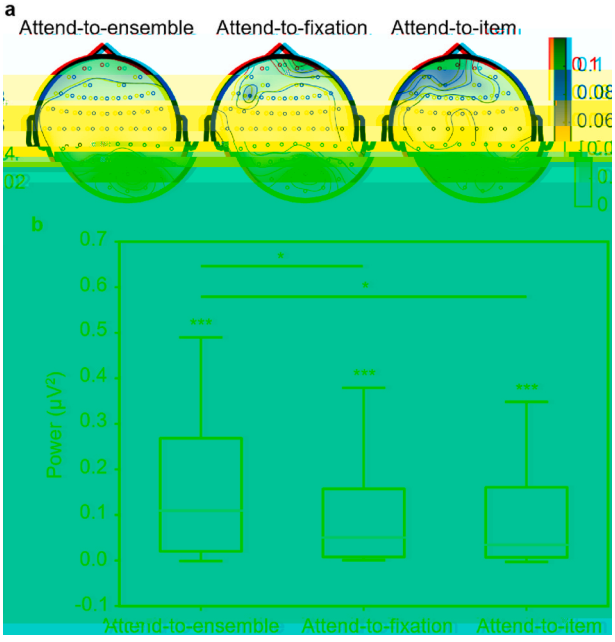

Fig. 4. Attentional effect on the SSVEP to the ensemble size. **a**. Topographies of the SSVEP power in the three attention conditions. **b**. SSVEP power at POz in the three attention conditions. ***$p < 0.001$, *$p < 0.0$.

ore importantly, the SSVEP power was significantly greater in the attend-to-ensemble condition than in the attend-to-fixation ($W = 210$, $p = 0.011$, $r_{rb} = 0.11$) and attend-to-item ($W = 21$, $p = 0.011$, $r_{rb} = 0.1$) conditions. No significant difference was found between the attend-to-fixation and the attend-to-item conditions ($W = 170$, $p = 0.\ 9$, $r_{rb} = 0.\ $). These results are consistent with the attentional effect on ensemble perception at the behavioral level (Baek and Chong, 2020a; Chong and Treisman, 200 b; de Fockert and archant, 200) and demonstrate that distributed attention over the global pattern enhances the specialized brain response to the ensemble size.

3.4. Attentional effects on the contributions of individual circle sizes, local interactions, and global interaction to the ensemble size perception

The manipulation of attention also allowed to examine how attentional distribution over the circle array affects the neural representations of the individual circle sizes, the local interactions, and the global interaction, as well as their contributions to the SSVEP. As in Experiment 1, we calculated the predicted accuracy differences between the full model and the three reduced models. The same five electrodes as in Experiment 1 were selected for statistical analyses. We found that the neural representation of the individual sizes was significant in all three attention conditions (Fig. a, all $ps < 0.001$), with no cross-condition differences (all $ps > 0.0$). Similarly, the neural representation of the local interactions was significant in all three conditions (Fig. b, all $ps < 0.01$), with no cross-condition differences (all $ps > 0.0$). However, the neural representation of the global interaction exhibited a different pattern (Fig. c). While the neural representation of the global interaction was significantly above zero in the attend-to-ensemble condition ($W = 2\ .00$, $p < 0.001$, $r_{rb} = 1.00$), it was not different from zero in the attend-to-fixation condition ($W = 9.00$, $p = 0.70$, $r_{rb} = -0.\ 0$) and even significantly below zero in the attend-to-item condition ($W = 1.00$, $p < 0.001$, $r_{rb} = -0.1$). Importantly, the neural representation of the global interaction in the attend-to-ensemble condition was significantly greater than those in the attend-to-fixation ($W = 2\ 9.00$, $p < 0.001$, $r_{rb} = 0.90$) and the attend-to-item ($W = 2\ 2.00$, $p < 0.001$, $r_{rb} = 0.99$) conditions, and there was no significant difference between the attend-to-fixation and the attend-to-item conditions ($W = 179.00$, $p =$

0.27 , r_{rb} = 0. 2). These results demonstrated that the neural representations of the individual circle sizes and the local interactions were not modulated by the attentional distribution. In contrast, the neural representation of the global interaction could be enhanced by distributed attention on the global pattern.

Next, we directly examined how the contributions of the neural representation of the individual circle sizes, the local interactions, and the global interaction to the ensemble size perception were modulated by attention. We compared the SSVEP power of the predicted EEG signal in the full model with those in the three reduced models. As shown in Fig. 1, the neural representation of the individual sizes and the local interactions did not contribute significantly to the SSVEP power in all three attention conditions (all *ps* > 0.0). In contrast, the neural representation of the global interaction contributed significantly to the SSVEP power in the attend-to-ensemble (W = 2 .00, $p < 0.001$, r_{rb} = 0.[illegible]1) and attend-to-fixation conditions (W = 211.00, $p = 0.01$, r_{rb} = 0.17), but not in the attend-to-item condition (W = 117.00, $p = 1$, r_{rb} = −0.0[illegible]). The contribution of the global interaction was significantly greater in the attend-to-ensemble condition than in the attend-to-item condition (W = 20 .00, p = 0.0 1, r_{rb} ∈ 0.11), demonstrating that attention to the ensemble enhanced the contribution of the global interaction to the ensemble size perception.

4. Discussion

We used a frequency-tagging technique, steady-state visual evoked potential (SSVEP), in combination with the temporal response function (TRF) technique, to study the neural signature and computational principle of ensemble size representation. Our findings provided evidence for a global mechanism of ensemble perception. Specifically, first, SSVEP showed clear electrophysiological responses that were synchronized with the frequency of the mean size changes, revealing that the human brain has a specialized neural response to ensemble size perception; second, using the TRF approach to predict EEG responses to individual sizes and their local and global interactions, we identified that the global interaction of all items in the display was encoded in EEG signals and contributed directly and significantly to ensemble size perception; finally, we identified, for the first time, that the attentional enhancement effects on ensemble perception were accompanied with an increased contribution only from the global interaction component, suggesting that the attentional enhancement on ensemble size perception derives from the effect of attention on the global interaction processing. Together, our findings support a specialized and global neural mechanism for ensemble size perception and suggest that the global interaction over all individuals contributes to ensemble size perception.

The existence of a specialized and global neural mechanism for ensemble perception is much debated. The subsampling hypothesis argues that ensemble size can be accurately estimated by randomly sampling and linearly averaging a few items strategically (yczek and Simons, 200[illegible]; Solomon et al., 2011). However, this would not predict the EEG signals synchronized with the base frequency, which results from the variation of the mean size rather than combinations of a subset of individual items. Furthermore, the subsampling hypothesis could not explain the global interaction result, i.e., the interaction of all items contributed to

linearization (e.g., simple averaging) could not generate efficient ensemble perception. Recent studies have demonstrated that the contributions of individuals are weighted in their mean (Choi and Chong, 2020) and variance (Jeong and Chong, 2021) computations for ensemble perception. Thus, these models and ours commonly suggest that ensemble perception is not achieved by simple averaging. However, because the present study did not manipulate the weights of individual circles and our TRF method could not compute the weights of individual circles in single trials, the current results could not examine the contribution of weighted averaging in ensemble perception. The global interaction component does not exclude the effect of weighted averaging either.

Intuitively, the ensemble size can be computed in a hierarchically connected, feedforward neural network. In this framework, low-level processing (i.e., the processing of individuals) determines high-level processing (i.e., the processing of the ensemble), and the representations of individual sizes are independent of each other. However, this pure feedforward framework does not explain the present results that the contribution of the representations of individuals to the ensemble size perception is not significant. It does not accommodate previous findings that the representations of individuals were degraded in ensemble perception (Allik et al., 201 , 201 ; Ariely, 2001), either. The present results advocate recurrent computations (Edelman and Gally, 201 ; Jastrzębowska et al., 2021; Lamme and Roelfsema, 2000; Singer, 2021) in ensemble size perceptionfi s

excu rrent con se ofwieyt- gudanin

Ding, N., Simon, J. ., 2012. Neural coding of continuous speech in auditory cortex during monaural and dichotic listening. J. Neurophysiol. 107, 7[illegible]–[illegible]9. https: doi.org 10.11 2 n.00297.2011.
Edelman, G. ., Gally, J.A., 201 . Reentry: a key mechanism for integration of brain function. Front. Integr. Neurosci. 7 https: doi.org 10. [illegible]9 fnint.201 .0001 .
Epstein, .L., Emmanouil, T.A., 2021. Ensemble statistics can Be available before individual item properties: electroencephalography evidence using the oddball paradigm. J. Cognit. Neurosci. , 10 1–101[illegible]. https: doi.org 10.1112 ocn a 0170 .
Frost, J., 2019. Regression Analysis: an Intuitive Guide for sing and Interpreting Linear odels. James D. Frost.
Gordon, N., Hohwy, J., Davidson, .J., van Boxtel, J.J.A., Tsuchiya, N., 2019. From intermodulation components to visual perception and cognition-a review. Neuroimage 199, [illegible]0– 9 . https: doi.org 10.1011 .neuroimage.2019.01.00[illegible].
Haberman, J., Whitney, D., 2007. Rapid extraction of mean emotion and gender from sets of faces. Curr. Biol. 17, R7 1–R7 . https: doi.org 10.1011 . cub.2007.01.0 9.
Hock, H.S., Schöner, G., 2011. Nonlinear dynamics in the perceptual grouping of connected surfaces. Vis. Res. 121, [illegible]0–91. https: doi.org 10.1011 . visres.201 .01.001.
Iakovlev, A. ., tochkin, I.S., 2021. Roles of saliency and set size in ensemble averaging. Atten. Percept. Psychophys. [illegible] , 12 1–1212. https: doi.org 10. 7 [illegible] s1 1 -020-020[illegible]9-w.
Im, H.Y., Albohn, D.N., Steiner, T.G., Cushing, C.A., Adams, R.B., veraga, ., 2017. Differential hemispheric and visual stream contributions to ensemble coding of crowd emotion. Nat. Human Behav. 1, [illegible]2[illegible]–[illegible] 2. https: doi.org 10.10 [illegible] s 1 12-017-022 -z.
Jastrzębowska, .A., Chicherov, V., Draganski, B., Herzog, .H., 2021. nraveling brain interactions in vision: the example of crowding. Neuroimage 2 0, 11[illegible] 90. https: doi.org 10.1011 .neuroimage.2021.11[illegible] 90.
Jeong, J., Chong, S.C., 2021. Perceived variability re ects the reliability of individual items. Vis. Res. 1[illegible] , 91–10 . https: doi.org 10.1011 .visres.2021.02.00[illegible].
Jia, J., Fang, F., Luo, H., 2019. Selective spatial attention involves two alpha-band components associated with distinct spatiotemporal and functional characteristics. Neuroimage 199, 22[illegible]–2 1. https: doi.org 10.1011 .neuroimage.2019.0 .079.
Jia, J., Liu, L., Fang, F., Luo, H., 2017. Sequential sampling of visual ob ects during sustained attention. PLoS Biol. 1 , e200190 https: doi.org 10.1 71 ournal. pbio.200190 .
im, S.S., Gomez-Ramirez, ., Thakur, P.H., Hsiao, S.S., 201 . ultimodal interactions between proprioceptive and cutaneous signals in primary somatosensory cortex. Neuron [illegible]1, – 11. https: doi.org 10.1011 .neuron.201 .0 .020.
Lalor, E.C., Pearlmutter, B.A., Reilly, R.B., cDarby, G., Foxe, J.J., 2001. The VESPA: a method for the rapid estimation of a visual evoked potential. Neuroimage 2, 1 9–1 11. https: doi.org 10.1011 .neuroimage.2001.0 .0 .
Lamme, V.A.F., Roelfsema, P.R., 2000. The distinct modes of vision offered by feedforward and recurrent processing. Trends Neurosci. 2 , 71– 79. https: doi.org 10.1011 S0111-22 1(00)011 7- .
Leib, A.Y., osovicheva, A., Whitney, D., 2011. Fast ensemble representations for abstract visual impressions. Nat. Commun. 7, 1 1[illegible]1 https: doi.org 10.10 [illegible] ncomms1 1[illegible]1.
Luck, S.J., Vogel, E. ., 1997. The capacity of visual working memory for features and con unctions. Nature 90, 279–2[illegible]1.
eigen, T., Bach, ., 2000. On the statistical significance of electrophysiological steady-state responses. Doc. Ophthalmol. 9[illegible], 207–2 2.
yczek, ., Simons, D.J., 200[illegible]. Better than average: alternatives to statistical summary representations for rapid udgments of average size. Percept. Psychophys. 70, 772–7[illegible][illegible]. https: doi.org 10.10 [illegible] fi. PP.70. .772.
Neumann, .F., Schweinberger, S.R., Burton, A. ., 201 . Viewers extract mean and individual identity from sets of famous faces. Cognition 12[illegible], 1–1 . https: doi.org 10.1011 .cognition.201 .0 .001.
Norcia, A. ., Appelbaum, L.G., Ales, J. ., Cottereau, B.R., Rossion, B., 201 . The steady-state visual evoked potential in vision research: a review. J. Vis. 1 , . https: doi.org 10.1117 1 .1. .r Vi ia; Na r
Oh, B.-I., im, Y.-J., ang, .-S., 2019. Ensemble representations A em;
ponra im r B.R.x